



CA1000427

Atomic Energy of Canada Limited

**MICROPROBE DETERMINATION OF
THE $\alpha/(\alpha+\beta)$ BOUNDARY FOR THE ZR-NB SYSTEM**

by

(MRS.) I. T. BETHUNE and C. D. WILLIAMS

Chalk River, Ontario

July, 1968

AECL-2715

MICROPROBE DETERMINATION OF THE $\alpha/(\alpha+\beta)$ BOUNDARY
FOR THE ZR-NB SYSTEM

by

(Mrs.) I.T. Bethune and C.D. Williams

ABSTRACT

Electron probe microanalysis has been used to locate the position of the $\alpha/(\alpha+\beta)$ boundary in the Zr-Nb phase diagram by measuring the phase compositions in specimens of a Zr-2.5 wt.% Nb-0.12 wt% O alloy annealed at temperatures in the range 600-850°C. The solubility of Nb in α -Zr at 600°C is shown to be 1.1 ± 0.1 wt.%. The concentration of Nb in the α -phase annealed for short intervals at 850°C is also close to 1%, decreasing to 0.85 ± 0.05 wt.% with prolonged annealing at this temperature. A precise determination of the $(\alpha+\beta)/\beta$ boundary has not been made; extrapolation of non-equilibrium compositions indicate that the monotectoid composition is close to 20 wt.% Nb, as shown in earlier phase diagram work.

Chalk River Nuclear Laboratories
Chalk River, Ontario

July, 1968.

AECL-2715

MICROPROBE DETERMINATION OF THE $\alpha/(\alpha+\beta)$ BOUNDARY
FOR THE ZR-NB SYSTEM

by

(Mrs.) I.T. Bethune and C.D. Williams

INTRODUCTION

One of the alloys used for fuel cladding and pressure tube applications in water cooled reactors is Zr-2.5% Nb which can be substantially strengthened by heat treatment. On rapid cooling from the β range, the martensitic α' phase is obtained with Nb retained in super-saturated solid solution. Pretreatment in the $\alpha+\beta$ range results in a duplex structure consisting of islands of α in a matrix of α' . The α' phase is subject to age hardening during post-quenching treatments at 500°C (1) (2). There is considerable interest in the Nb content of these phases since the strength, corrosion resistance, and response of the phases to irradiation have been shown to be a function of Nb content and distribution (1) (2) (3).

It was the aim of this work, therefore, to investigate the Nb content of the α and α' phases in the Zr-2.5% Nb alloy and to determine the location of the $\alpha/(\alpha+\beta)$ phase boundary. The location of this boundary and in particular the solubility of Nb in α -Zr near both the eutectoid temperature and currently useful solution treatment temperatures have not been unambiguously identified in previous work. In part this has been due to the difficulty of measuring Nb concentrations in dilute solutions in α -Zr by lattice parameter methods. For example, Klepfer (4), using X-ray diffraction analysis, was unable to detect any Nb in a 1.4% Nb alloy, even after annealing 500 hours below the eutectoid temperature. The electron probe microanalyzer under ideal conditions, is capable of detecting elements well below 1 wt.% and was used to measure the composition of phases after a grain size of $> 5 \mu\text{m}$ was achieved by appropriate deformation/thermal treatments.

The Zr-Nb Phase Diagram; Published Information

The Zirconium-Niobium equilibrium diagram derived by Lundin and Cox (5) is given in Figure 1. The diagram shows a monotectoid reaction, $\beta_{\text{Zr}} \rightarrow \alpha_{\text{Zr}} + \beta_{\text{Nb}}$ at 610°C and 20% Nb and a

monotectoid loop of the two solid solutions β_{Zr} and β_{Nb} occurs below 970°C.

There is controversy in the literature as to the exact position of the monotectoid point and to the solubility limit of Nb in α -Zr at this monotectoid level, shown at 0.6 wt.% by Lundin and Cox. The diagram according to Rogers and Atkins⁽⁶⁾ contained a monotectoid horizontal at 600°C with the monotectoid point at 17.5% Nb, the maximum solubility of Nb in α -Zr being 6.4%. Earlier work by Hodge⁽⁷⁾ indicated that the monotectoid lay at 625°C and 10% Nb and that the solubility of Nb in α -Zr at 625°C was 6%. According to Ivanov⁽⁸⁾ the solid solubility limit of Nb in α -Zr is 1.5%. Bichkov⁽⁹⁾ using dilatometric techniques placed the monotectoid at 560°C and 12% Nb, whereas Knapton⁽¹⁰⁾ who employed chiefly metallographic techniques placed it at 610°C and 20% Nb and the Nb solubility in α -Zr at less than 1 at %.

The most recent work has been reported by Richter et al⁽¹¹⁾ who found the location of the monotectoid point and the maximum solubility of Nb in α -Zr to be dependent upon the oxygen concentration present in the alloy. Their phase diagram for sponge zirconium is shown in Figure 2. Richter et al considered that the oxygen concentration present even in iodide Zr, leads to a distinct ternary Zr-Nb-O character, and they found the solubility of Nb in α -Zr to be between 1.5 and 2.0 wt.%, the actual value being dependent on the oxygen content.

Oxygen is known to raise the $(\alpha+\beta)/\beta$ transformation temperature in Zr; the extent of this effect on the Zr-2.5 wt.% Nb alloy has been reported by Paton⁽¹²⁾ and Foley et al⁽¹³⁾. The α - β transformation temperature in pure zirconium is raised from 862°C to 920°C by the presence of 1200 ppm oxygen.

Slattery⁽¹⁴⁾ noted that the high values derived for solid solubilities of Nb in α -Zr are associated with the use of 'dynamic' techniques such as electrical resistivity and dilatometry which involve the interpretation of curves, whereas the lower values have been obtained by static methods, i.e., X-ray diffraction and metallography. The low value of 560°C for the monotectoid temperature was also obtained dilatometrically.

Material and Specimen Preparation

The alloy used was a commercial alloy, produced by the

Wah Chang Corporation, containing 2.7 wt.% Nb and 0.137 wt.% O. Initially the material was in the form of cold-rolled sheet of thickness 0.065 inches. Table 1 gives the manufacturer's analysis of principal impurities present.

The following stress-annealing procedure was used to provide specimens having an α -grain size sufficiently large ($>5\ \mu\text{m}$ diameter) to permit accurate probe analysis:-

strips of the cold-rolled sheet were further cold-rolled to reductions of 34% and 68%, and were vacuum-annealed for intervals in the range 1-672 hours at temperatures in the range 600-850°C. All homogenization treatments were terminated by quenching into water. Additional material was given cold reduction in the range 40-60% to provide specimens of adequate grain size after annealing at temperatures below 700°C.

Table 2 shows the α -grain sizes achieved after each anneal; although the α grain diameters above the broken line were large enough for analysis the transformed β areas were too small for analysis in all specimens except those above the solid line.

Microprobe Examination

After the preliminary metallographic evaluation of grain size the specimens were repolished to remove the effect of the etchant and to achieve as flat a surface as possible, prior to the probe examination. (All specimens were mounted in Woods alloy to provide the necessary conducting mount).

Quantitative microprobe analysis was carried out using an Associated Electrical Industries S.E.M.2 to determine the amount of Nb and Zr in the α and β (or transformed β) phases existing in the material after heat treatment. The instrument was operated with an excitation potential of 20 kv and a probe current of 0.2 μA ; conditions were optimized for the detection of Nb and Zr with the aid of pure standards of the two metals. The electron and X-ray images shown in Figure 3 illustrate the extent to which the probe was able to qualitatively display the segregation of Nb in the β component of the alloys. Peak-to-background ratio measurements for the ZrL α and NbL α lines were made in both phases in each specimen. Comparison of these intensity measurements with those from pure metals provided relative intensities which were converted into weight fractions. To allow for the non-linearity which exists in the

relation between composition and X-ray intensity due to matrix absorption and differences in atomic number of the component elements, corrections to the measured intensities were necessary. A short computer program was written in Fortran to evaluate compositions corrected for both absorption and atomic number effects using the correction procedure of Philibert⁽¹⁵⁾ and μ/p values of Heinrich⁽¹⁶⁾. The corrected results are shown with the measured values in Table 3.

Volume of the α -Phase

Specimens annealed at 650°C, 750°C and 850°C were examined using a quantitative television microscope to determine the volume fraction of the α -phase present. These values were used with the compositions of the phases determined by probe analysis to provide a check on the consistency of the data. Table 4 includes the α -volumes and calculated alloy compositions based on the pertinent phase analysis. It is noted that a satisfactory correlation is obtained between phase analysis and volume, and total alloy composition.

Location of the $\alpha/(\alpha+\beta)/\beta$ Phase Boundaries

The experimental values for Nb concentrations in the α - and β - phases have been plotted against homogenization temperature, Figure 4, to give locations for the $\alpha/(\alpha+\beta)$ and $(\alpha+\beta)/\beta$ boundaries. As the variations in analyses for specimens annealed for different times have shown, Table 3 and Figure 4, the α and β phases were not in perfect equilibrium although the α -phase compositions showed a much smaller variation than those of the β phase. Thus, the $(\alpha+\beta)/\beta$ boundary shown in Figure 4 cannot be considered to be the equilibrium boundary; however the monotectoid composition is evidently >17 wt.% Nb, as shown in earlier work⁽⁶⁾⁽¹⁰⁾⁽¹¹⁾. The location of the $\alpha/\alpha+\beta$ boundary as shown is considered to be satisfactorily established for the alloy used; in particular the location is valid for estimation of α -phase compositions in alloys subjected to conventional short homogenization treatments at temperatures below the $(\alpha+\beta)/\beta$ transus.

The value obtained here for solubility of the Nb in α -Zr at 600°C is 1.1 ± 0.1 wt.% and lies between the values given by Lundin and Cox⁽⁵⁾ Figure 1, and Richter et al⁽¹¹⁾, Figure 2.

Table 5 includes a summary of corresponding data available in the literature. The temperatures corresponding to the maximum solubility data in the work due to Lundin and Cox⁽⁵⁾ and Richter et al⁽⁶⁾ were 610°C and 590°C respectively, and 600°C for the present work. There has been no indication in our work that the solubility increases significantly over the measured value of 1.1 wt.% in this temperature range. Richter et al⁽⁶⁾ noted that as the purity of the alloys decreased the solubility of niobium in α -zirconium also decreased. The present results are consistent with those of Richter et al⁽⁶⁾ when the pertinent oxygen concentrations are considered, although the solubility value of 0.6 wt.% obtained by Lundin and Cox⁽⁵⁾ is anomalously low. No support is found in the present work for the high solubility value obtained by Hodge⁽¹⁾ and Rogers and Atkins⁽²⁾.

REFERENCES

- (1) Ells, C.E., Dalgaard, S.B., Evans, W., and Thomas, W.R., Proceedings 3rd International Conference on Peaceful Uses of Atomic Energy, Geneva, AECL-2022 (1964).
- (2) Winton, J., and Murgatroyd, R.A., Zirconium and its Alloys, p. 358, Electrochemical Society, Buffalo Conf. (1966).
- (3) Williams, C.D., and Ells, C.E., Phil. Mag., to be published (1968).
- (4) Klepfer, H.H., J. Nucl. Materials, 9, p. 65 (1963).
- (5) Lundin, C.E., and Cox, R.H., USAEC, Report No. 1/AT(11-1)-752 (1960).
- (6) Rogers, B.A., and Atkins, D.F., Trans. AIME 203, p. 1034 (1955).
- (7) Hodge, E.S., TID-5061, 461 (1952).
- (8) Ivanov, O.S., and Grigorovich, V.K., Proc. 2nd Int. Conf. Peaceful Uses of Atomic Energy, Geneva, 1958, Vol. 5, p. 34 (P/2046).
- (9) Bichkov, Y.F., J. Nucl. Energy, 5, p. 402 (1957).
- (10) Knapton, A.G., J. Less Common Metals, 2, p. 113 (1960).
- (11) Richter, H., Wincierz, P., Anderko, K., and Zwicker, U., J. Less Common Metals, 4, p. 252 (1962).
- (12) Paton, N., and Osadchuk, R., Paper presented at Conference of Metallurgists, Montreal (1964).
- (13) Kench, J.R., Foley, J.H., and Aldridge, S.A., AECL-2623 (1966).
- (14) Slattery, G.F., Zirconium and Its Alloys', p. 336, Electrochemical Society, Buffalo Conf. (1966).
- (15) Philibert, J., 3rd International Symposium on X-ray Optics and X-ray Microanalysis, p. 379, Academic Press (1963).

REFERENCES (Continued)

- (16) Heinrich, K.F.J. 'The Electron Microscope', p. 296,
Wiley (1966).

Table 1

Manufacturer's Analysis of the Zr-2.7 wt.%Nb-0.137 wt.%O Alloy

Used in Microprobe Experiments to Determine the

$\alpha/(\alpha+\beta)$ Boundary

<u>Element</u>	<u>Impurity Content, ppm</u>
Al	45
C	160
Cr	130
Cu	< 25
Fe	900
Hf	< 46
N	63
Si	51
Ta	< 200
Ti	< 50
W	40
Zr	< 50
Others	< 83 total

Table 2

α -grain Size in Stress-annealed Specimens

Grain size in μm

Annealing Time - hours	1			24			65			168	192	672
% Cold Reduction	0	34	68	0	34	68	50	55	60	68	68	68
Annealing Temp., °C												
850	5	5	5	15	15	15	-	-	-	-	20	-
800	3	3	3	7	7	7	-	-	-	15	-	-
750	3	3	3	10	10	10	-	-	-	-	-	-
700	<2	<2	<2	<2	<2	5	5	7	-	-	-	18
650	<2	<2	<2	<2	<2	5	6	7	-	-	-	12
600	<2	<2	<2	<2	<2	2	5	8	8	-	-	-

TABLE 3

ANALYSES OF α - AND β -PHASES IN STRESS ANNEALED SPECIMENS

Annealing Temp. °C	Prior Reduction %	Annealing Time Hours	α -phase Analysis				β -phase Analysis			
			(i) Nb	(ii) Nb	(iii) Zr	Total	(i) Nb	(ii) Nb	(iii) Zr	Total
			Uncorrected	Corrected	Uncorrected	(ii) + (iii)	Uncorrected	Corrected	Uncorrected	(ii) + (iii)
850°	0	1	1.08	1.02	95.87	96.89	3.18	3.01	94.53	97.54
	34	1	1.02	0.97	98.58	99.55	3.06	2.92	97.52	100.44
	68	1	1.01	0.95	96.76	97.71	3.08	2.93	95.73	98.66
	68	24	0.95	0.90	99.08	99.98	3.09	2.95	97.67	100.62
	68	192	0.87	0.83	98.70	99.53	3.90	3.72	96.90	100.62
800°	0	24	1.12	1.06	97.54	98.60	3.18	3.02	96.63	99.65
	34	24	1.03	0.98	98.91	99.89	3.89	3.72	97.30	101.02
	68	24	1.19	1.13	99.07	100.20	3.91	3.74	97.59	101.33
	68	168	0.84	0.80	98.30	99.10	5.20	4.98	96.40	101.38
750°	0	24	1.13	1.07	97.75	98.82	5.97	5.70	94.47	100.17
	34	24	1.18	1.12	98.31	99.43	5.84	5.59	95.44	101.03
	68	24	1.21	1.14	97.07	98.21	6.52	6.27	96.37	102.64
700°	55	65	1.17	1.11	98.84	99.95	8.30	7.92	92.06	99.98
	68	672	1.05	1.00	99.60	100.60	11.06	10.53	88.40	98.93
	68	672	1.20	1.15	99.80	100.95	12.20	11.61	87.20	98.81
650°	55	65	1.04	0.99	98.12	99.11	9.70	9.33	92.87	102.20
	55	65	0.90	0.86	99.80	100.66	9.58	9.24	93.80	103.04
	68	672	1.20	1.15	99.70	100.85	14.80	14.28	88.20	102.48
600°	55	65	1.22	1.16	98.51	99.67	11.06	10.43	85.76	96.19
	55	65	1.04	0.99	99.71	100.70	10.74	10.44	94.77	105.21
	60	65	1.19	1.13	98.01	<u>99.14</u>	11.14	10.70	90.77	<u>101.47</u>
Mean value = 99.48									Mean value = 100.64	
<u>Combined mean = 100.06</u>										

TABLE 4

Alloy Composition Calculated From α -phase Volume
Measurements and Phase Analyses

Net Nb Concentration = 2.7 wt.% from Chemical Analysis

Specimen Treatment	Volume % α -phase	Measured Nb Concentration		Calculated Total Nb Concentration wt.%
		α -phase	β -phase	
68% reduction 24 hours at 850°C	20.9	0.9	2.9	2.5
34% reduction 24 hours at 750°C	64.1	1.1	5.6	2.7
55% reduction 65 hours at 650°C	77.4	0.9	9.2	2.8

Table 5

Summary of Analyses of Niobium Solubility in α -zirconium

Source	Alloy Purity	Method of Analysis	Maximum Solubility of Nb in α -Zr
Hodge (7)	Sponge Zr base	Metallography	6.0 wt.%
Rogers and Atkins (6)	Iodide Zr	Electrical resistivity, dilatometry	6.4 wt.%
Ivanov et al (8)	Iodide Zr	Metallography X-ray analysis	1.5 wt.%
Knapton(10)		Metallography	< 1.0 wt.%
Lundin and Cox(5)	Iodide Zr 0.017 wt.% O ₂	Metallography	0.6 wt.%
Richter et al(11)	Iodide Zr 0.080 wt.% O ₂	Metallography Electrical resistivity	1.7 wt.%
Present Work	Sponge Zr base 0.137 wt.%O ₂	Probe analysis	1.1 \pm 0.1 wt.%

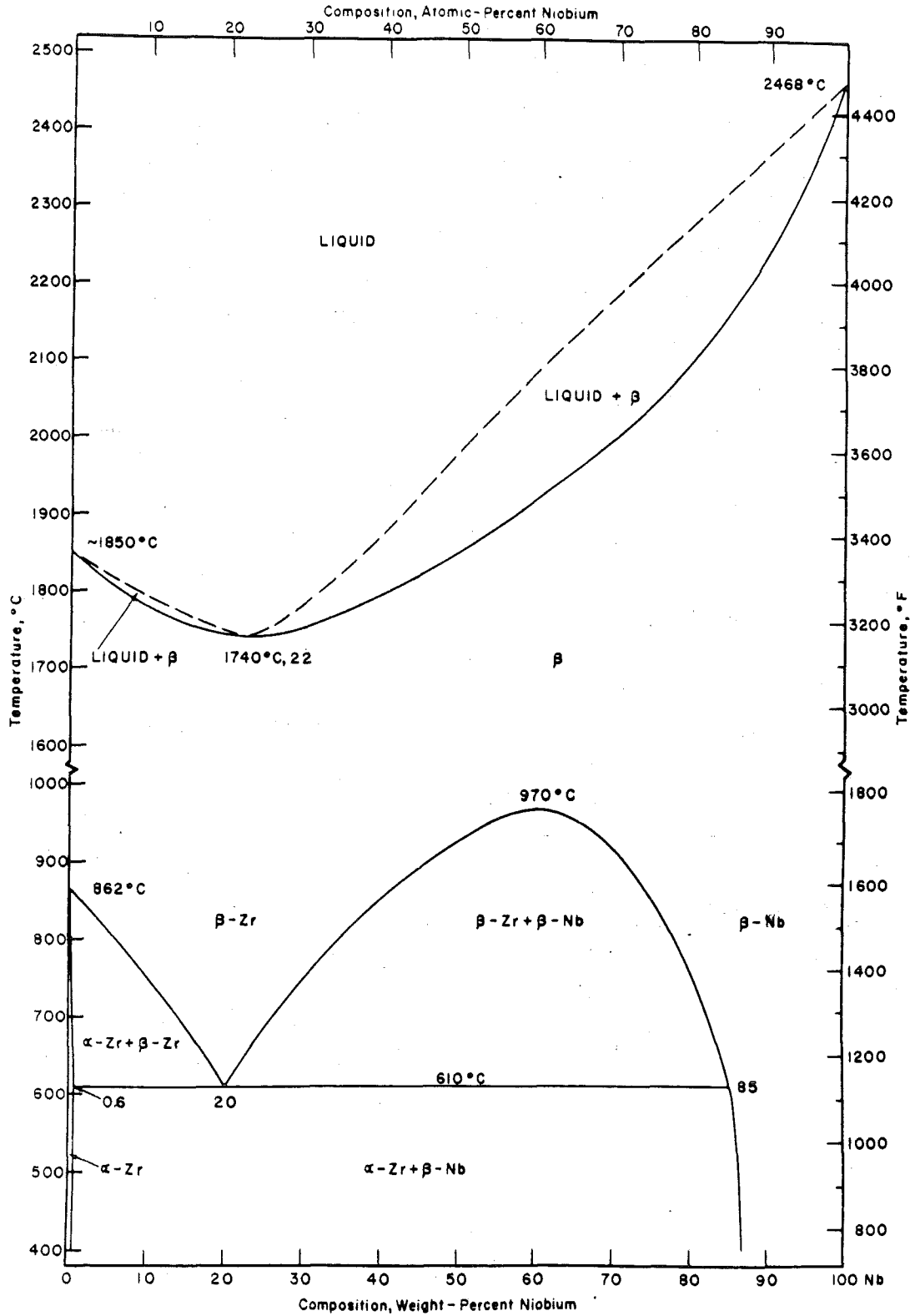


FIG - 1

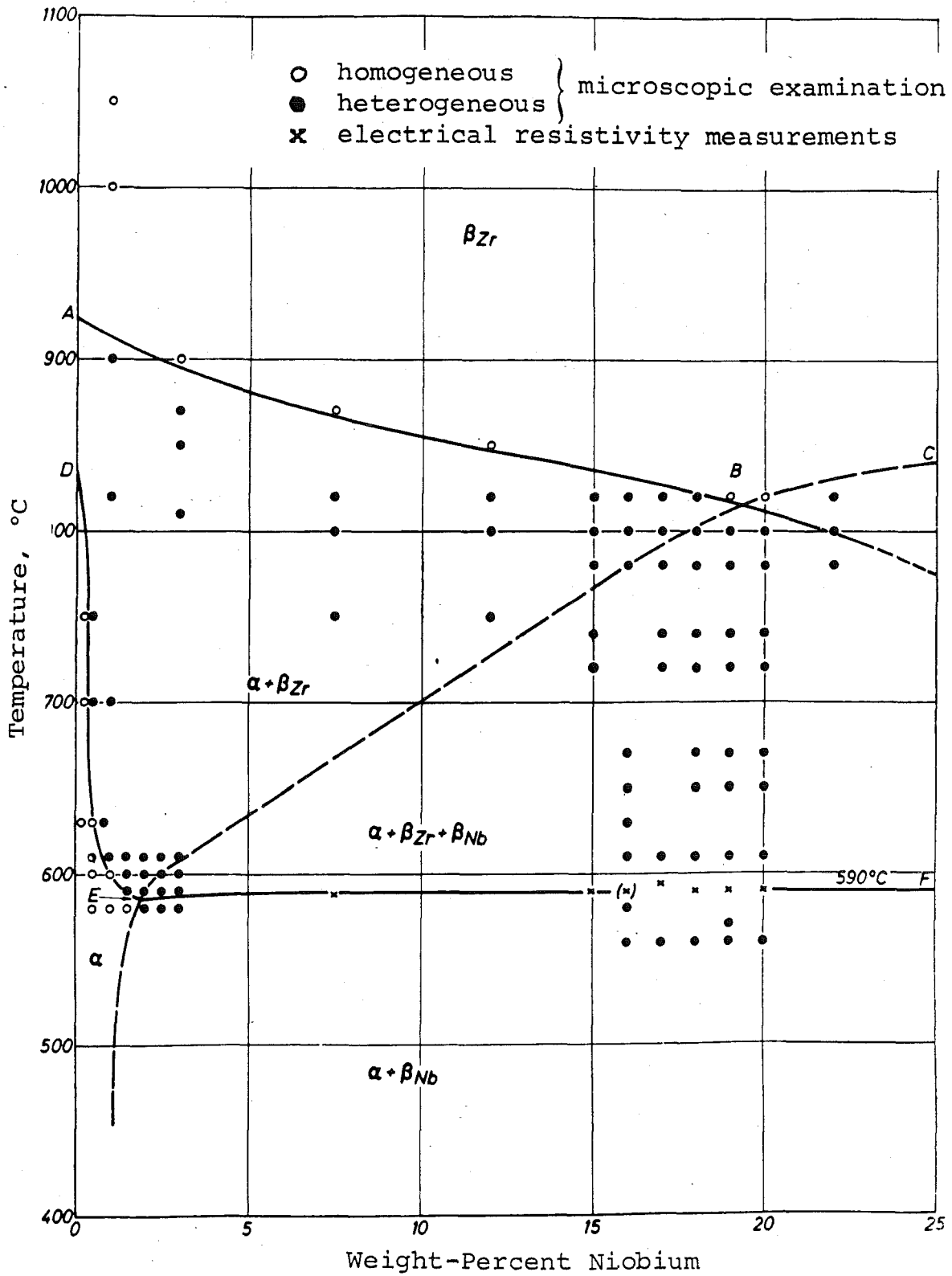
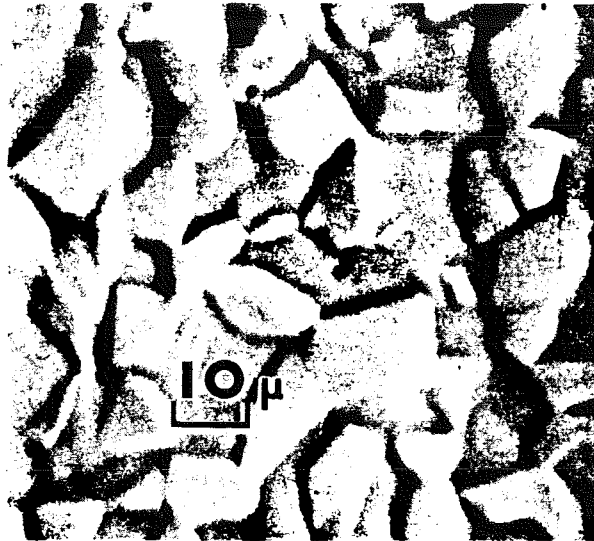
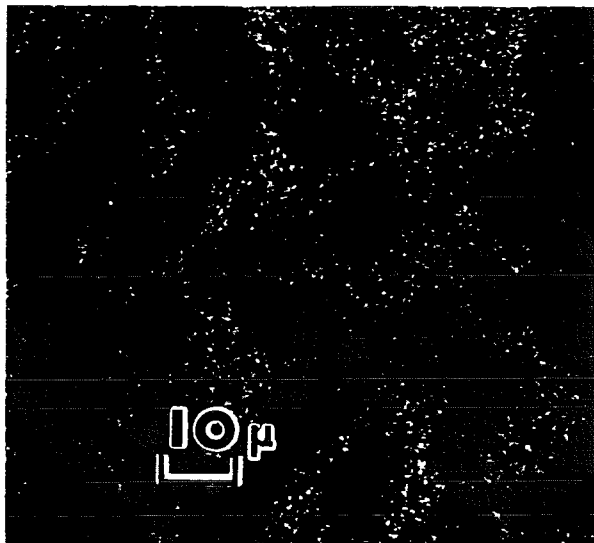


FIG - 2



Electron Image
showing α grains in a matrix of transformed β



NbL α X-ray Image
The light shaded areas are the Nb-rich (trans-
formed β) phase

FIGURE 3

Zr-2.5% Nb, 168 hours at 800°C. Electron and X-ray images showing qualitatively the distribution of Nb in the β -phase areas.

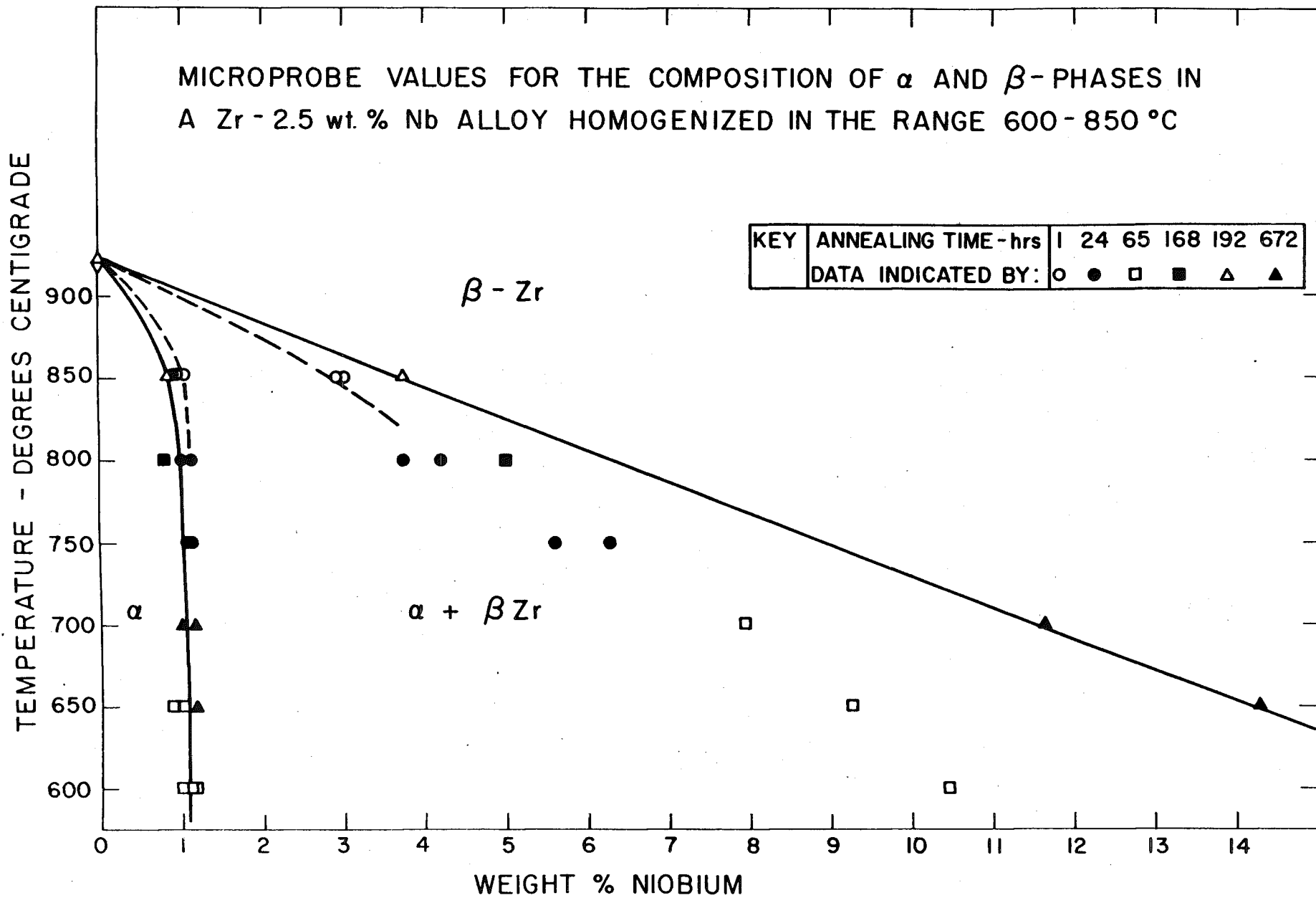


FIG - 4